

Stiff equation of state for a holographic nuclear matter as instanton gas

†Kazuo Ghoroku¹, †Kouji Kashiwa², Yoshimasa Nakano³,
 §Motoi Tachibana⁴ and ‡Fumihiko Toyoda⁵

†Fukuoka Institute of Technology, Wajiro, Fukuoka 811-0295, Japan

§Department of Physics, Saga University, Saga 840-8502, Japan

‡Faculty of Humanity-Oriented Science and Engineering, Kinki University,
 Iizuka 820-8555, Japan

Abstract

In a holographic model, which was used to investigate the color superconducting phase of QCD, a dilute gas of instantons is introduced to study the nuclear matter. The free energy of the nuclear matter is computed as a function of the baryon chemical potential in the probe approximation. Then the equation of state is obtained at low temperature. Using the equation of state for the nuclear matter, the Tolman-Oppenheimer-Volkov equations for a cold compact star are solved. We find the mass-radius relation of the star, which is similar to the one for quark star. This result is understood from the stiffness and the large speed of sound of the instanton gas considered here.

¹gouroku@fit.ac.jp

²kashiwa@fit.ac.jp

³ynakano@kyudai.jp

⁴motoi@cc.saga-u.ac.jp

⁵fitoyoda@jcom.home.ne.jp

1 Introduction

Many analyses of the holographic quantum chromodynamics (QCD) imply a schematic phase diagram shown by Fig.1, where μ and T denote the chemical potential of quark and the temperature of the system, respectively. The solid curve represents the confinement/deconfinement transition, which is obtained as the Hawking-Page transition points from the AdS-soliton to the Reissner-Nordstrom background configurations through the following bulk action

$$S_{\text{Bulk}} = \int d^{d+1}x \sqrt{-g} \left\{ \mathcal{R} + \frac{d(d-1)}{L^2} - \frac{1}{4}F^2 \right\} \quad (1.1)$$

for $d = 5$ [1, 2]. We notice that, for the considering background of $d = 5$, the dimension of the boundary space-time is effectively 3+1 since one space dimension is compactified by the SHERK-SCHWARZ compactification. The above action has been firstly used to examine the electric superconductivity for $d = 3$ [3, 4, 5, 6, 7] and theory with R-symmetry for any d [8].

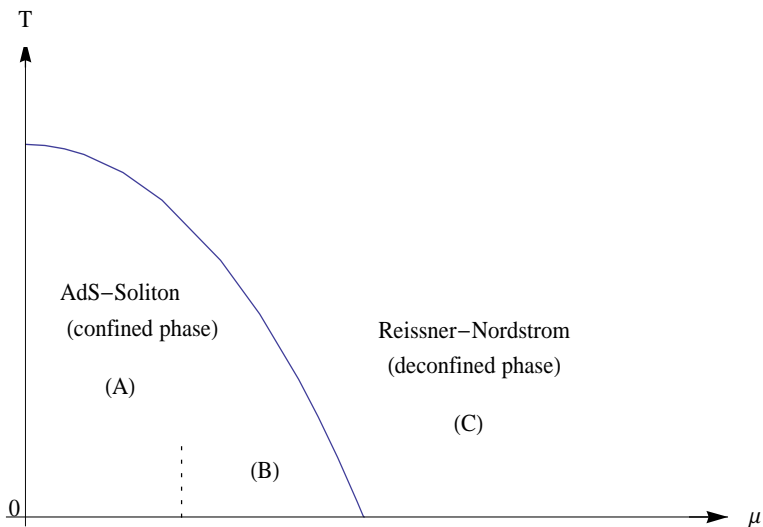


Fig. 1: A schematic phase diagram of QCD in (μ, T) plane.

Recently, Eq.(1.1) has been used as a bottom-up holographic QCD model to study color superconductivity [1, 2, 9, 10] in the region (C) of Fig.1. The analysis has been performed under the assumption that the $U(1)$ gauge field is dual to the baryon number current. The model is extended up to small N_c where N_c is the number of colors and the authors of Ref. [2] pointed out that the color superconducting (CSC) phase could not be found for $N_c \geq 2$. However, the existence of the CSC phase has been pointed out when the model is improved by adding the higher derivative terms, the Gauss-Bonnet term, to Eq.(1.1) [10].

Another point to be noticed is the dotted line shown in Fig. 1. In the confined phase (A), baryons are constructed from N_c quarks. Then, at a certain chemical potential, they are assembled as nuclear matter. The region (B) is called as the nuclear matter phase. In the previous studies, this phase has been foreseen in terms of the top-down model [11, 12, 13], based on the Sakai-Sugimoto D4/D8 model [14, 15]. In these models, baryon is introduced as an instanton which is a soliton constructed from the flavored vector mesons.

Here, based on our bottom-up holographic model (1.1), we study the nuclear matter according to the idea that it is constructed from the instanton gas. In order to provide baryons, we add $SU(N_f)$ gauge field sector to Eq.(1.1) [11, 14, 15, 16], where N_f is the number of flavors. Then the dilute gas of instantons is examined at finite chemical potential and at low temperature with Chern-Simons (CS) term which connects the instantons and the $U(1)$ gauge field [15]. From the model of the nuclear matter given here, we can derive the equation of state (EoS). Then it can be applied to the compact cold star like the neutron star to estimate the relation of the mass and the radius.

For the deconfined phase (C), up to now, some holographic models have been applied to investigate the neutron star with the core of quark matter [17, 18, 19]. On the other hand, the holographic investigation of the matter in the region (B) has not been performed well to study the neutron star.

In our approach, instead of solving the equations of motion, the flavored gauge fields are replaced by the instanton solution given in R^4 flat space with an instanton size ρ . The solution is regarded as a trial function of the solutions of their equations of motion. Since, in our case, the instanton is embedded in a deformed 4D space of the curved 6D background space-time, then the size ρ is not arbitrary, and it should be fixed at a suitable value [2, 15]. This value is determined here by minimizing the free energy of the system at $\rho = \rho_{\min}$. Then the other physical quantities (the free energy, the chemical potential, and others) are obtained by using this ρ_{\min} and other parameters of the theory. As a result, the resultant free energy can be expressed as a function of μ [2]. Then through this approach, we can obtain the EoS of the instanton gas, namely of the nuclear matter.

Another quantity which characterize the instanton gas is the speed of sound (C_s) of the system. We find the condition to its value as $1/2 < C_s^2 < 1$. Although it preserves the causality since it is smaller than unity, the lower bound is $1/2$, which is large as that of the nuclear matter.

In the next section, our bottom-up model is proposed by introducing a dilute gas of instantons. In Sec. 3, how to embed the instantons in the confined background metric is explained. In Sec. 4, the free energy of the system is computed according to our method, and EoS for the instanton gas is obtained at low temperature. In Sec. 5, using the EoS, the Tolman-Oppenheimer-Volkov (TOV) equations for a compact star are solved to find the mass-radius (M - R) relation. In Sec. 6, our results are compared with the ones from nuclear physics and astronomical observations. In the final section, summary and discussions are given.

2 Bottom-up CSC model with nuclear matter

We start from the bottom-up holographic model which is proposed as Yang-Mills (YM) theory with color superconducting phase. It is given by the following gravitational theory [2, 3, 4].

$$S = \int d^{d+1}\xi \sqrt{-g} \mathcal{L}, \quad (2.1)$$

$$\mathcal{L} = \mathcal{L}_{\text{Gravity}} + \mathcal{L}_{\text{CSC}}, \quad (2.2)$$

$$\mathcal{L}_{\text{Gravity}} = \mathcal{R} + \frac{d(d-1)}{L^2}, \quad (2.3)$$

$$\mathcal{L}_{\text{CSC}} = -\frac{1}{4}F^2 - |D_\mu \psi|^2 - m^2 |\psi|^2, \quad (2.4)$$

$$F_{\mu\nu} = \partial_\mu A_\nu - \partial_\nu A_\mu, \quad D_\mu \psi = (\partial_\mu - iqA_\mu)\psi. \quad (2.5)$$

It describes $d+1$ dimensional gravity coupled to a $U(1)$ gauge field, A_μ , and a charged scalar field, ψ . Here we consider the case of $d = 5$. The charge q denotes the baryon number of the scalar ψ , and it is chosen as $q = 2/N_c$ to represent the quark Cooper pair formation. The mass m is given to reproduce the corresponding conformal dimension of the diquark operator dual to the scalar field ψ with the charge $q = 2/N_c$. Here we put $1/2\kappa_6^2 = 1$, and the dimensionful $U(1)$ gauge coupling constant is set as unit. So the metric is dimension less and A_μ has dimension one as in the 3+1 dimensional case.

The above holographic model, previously, has been considered to be dual to the superconductor of the electric charge [3, 4] and of the R-charge [6]. And it is recently extended to a theory dual to the color superconductor in [1, 2, 9].

Here we add the sector of the $SU(N_f)$ gauge fields, which is used to build the nuclear matter through the instanton configuration, which generates the baryon number in QCD. The instanton configuration is here deformed since it is embedded in a higher dimensional curved space.

$$\mathcal{L} = \mathcal{L}_{\text{Gravity}} + \mathcal{L}_{\text{CSC}} + \mathcal{L}_{\text{V}}, \quad (2.6)$$

$$\mathcal{L}_{\text{V}} = -\frac{1}{4} \text{tr} F_{SU(N_f)}^2 \quad (2.7)$$

where $F_{SU(N_f)}^2$ denotes the 2-form $SU(N_f)$ gauge field. The coupling constant g_{YM}^2 is set as one. The mass dimension of the gauge field is taken to be one. Then, in order to pick up the coupling of the baryon number current and the instanton configuration, we add the CS term,

$$S = \int d^{d+1}x \sqrt{-g} \mathcal{L} + S_{\text{CS}}. \quad (2.8)$$

We notice that there are two ways to proceed the analysis based on this model since both the matter and the gravity fields are living in the same 6D space-time. Therefore, the matter fields are not confined to special D-branes. (i) So, in one way, we can solve the equations of motion of all fields, gauge fields and the gravity, in the same footing. In this case, the back-reaction of the gauge fields are included in the metric. (ii) On the

other hand, it is possible to restrict our calculation to the probe approximation where the equation of motion of the matter fields are solved on a fixed background given by the solution of the Einstein equations of $\mathcal{L}_{\text{Gravity}}$. This approximation is assured for the large gauge couplings.

Hereafter we proceed the analysis according to the probe approximation (ii). The matter parts are considered as the probe of the system. So firstly we fix the gravitational background by solving $\mathcal{L}_{\text{Gravity}}$.

2.1 Instanton in R^4

Before solving the equation of motion of our model, the ansatz for the $U(1)$ gauge field and the instanton configurations for $SU(2)$ gauge fields are given. The coordinates are denoted as $(\xi^0, \xi^1, \xi^2, \xi^3, \xi^4, \xi^5) = (x^0, x^1, x^2, x^3, w, z)$. Then, we make the ansatz for $U(1)$ gauge field as

$$A_b = A_b(z)\delta_b^0. \quad (2.9)$$

As for the $SU(2)$ vector fields, which are set as

$$\vec{f}_1 = F_{ab}^i \tau_i, \quad (2.10)$$

and the following ansatz are imposed,

$$(\vec{f}_1)_{ij} = Q(x^m - a^m, \rho) \epsilon_{ijk} \tau^k, \quad (2.11)$$

$$(\vec{f}_1)_{iz} = Q(x^m - a^m, \rho) \tau^i, \quad (2.12)$$

where ρ (a^m) denotes the instanton size (position), $\epsilon_{123z} = 1$, $i, j = 1, 2, 3$ and $m = 1, \dots, 4$, where $x^4 = z$. Then the $SU(N_f)$ vector part (2.7) is given for $N_f = 2$ as

$$\mathcal{L}_V = -\frac{3}{2}Q^2 \left[(g^{11})^2 + g^{11}g^{zz} \right]. \quad (2.13)$$

In order to see the baryon, Q is given as an instanton solution in flat 4D space $\{x^m\}$ [15],

$$Q = \frac{2\rho^2}{((x^m - a^m)^2 + \rho^2)^2}. \quad (2.14)$$

However, in general, this is not a solution of our bottom-up model since this configuration is embedded in a curved space. So, here, we introduce it as a trial function which is supposed to be a solution of the system under an appropriate condition. The trial function is given in our formulation such that the size parameter ρ of the instanton configuration is determined to satisfy the variational principle of the energy density in our bottom-up model. We determine it by minimizing the embedded instanton energy as in Refs. [13, 15]. We notice that there is an another method giving Q including its z dependence by solving the embedding equations of motion [12]. Here we solve only for the size parameter.

According to the above strategy, we study multi-baryon state by replacing $Q(z)$ by the multi-instanton form with dilute gas approximation. Then we rewrite Q as

$$Q^2 = \sum_i^{N_I} \frac{4\rho^4}{((x^m - a_i^m)^2 + \rho^2)^4}, \quad (2.15)$$

where the overlapping among the instantons are suppressed in obtaining Q^2 . This point is checked for our solutions.

In the case of the flat space, in R^4 , we find the energy density as a sum of each single instanton,

$$\begin{aligned} \int d^4\xi^m Q^2 &= 2N_I \int_0^\infty dz \bar{q}(z)^2 \\ &= \frac{2\pi^2}{3} N_I, \end{aligned} \quad (2.16)$$

where

$$\bar{q}^2 = \frac{\pi^2 \rho^4}{2(z^2 + \rho^2)^{5/2}} \quad (2.17)$$

for the case of dilute gas, where interactions between instantons are neglected. Then the result is given by one instanton ‘‘mass’’ times their number N_I .

In the present case, the instantons are embedded in a curved space. The metrics are the functions of the coordinate z . This implies that the state of the baryon is affected dynamically by the gluons. In other words, the baryon would be stable when it is embedded in the background corresponding to the confined phase. Furthermore, they would construct a nuclear matter like the neutron star as we see below.

3 Low temperature confined phase and the fourth coordinate z

We suppose the nuclear matter would be the gas of instantons made of the $SU(2)$ gauge fields in the confined phase. The space-time background solution, which is dual to the low temperature confined phase, is given from $\mathcal{L}_{\text{Gravity}}$ at low temperature as the AdS soliton solution. It is obtained as

$$ds^2 = r^2(\eta_{\mu\nu} dx^\mu dx^\nu + f(r) dw^2) + \frac{dr^2}{r^2 f(r)}, \quad (3.1)$$

where

$$f(r) = 1 - \left(\frac{r_0}{r}\right)^5, \quad r_0 = \frac{2}{5R_w}, \quad (3.2)$$

and $2\pi R_w$ denotes the compactified length of w , which denotes the coordinate of the compact S^1 . We should notice that this solution is also a back-reacted one when the

$SU(2)$ gauge fields are set to be zero. In this case, the phase diagram in the μ - T plane is given in Ref. [2].

Here we restrict the region of the parameters, T and μ , to the confined phase. In fact, under the configuration (3.1), one finds a linear potential between quark and anti-quark by evaluating the Wilson loop [20]. Hence the vacuum stays in the confined phase, and the instanton number is identified with the baryon number. Then, in this confined phase, we can examine the nuclear matter through the gas of instantons.

3.1 Coordinate z and embedding of instanton

In proceeding the analysis mentioned above, it is necessary to choose the coordinate z carefully. For example, we may choose the four coordinates to make the instanton as,

$$(\xi^0, \xi^1, \xi^2, \xi^3, \xi^4) = (x^0, x^1, x^2, x^3, r), \quad (3.3)$$

namely as $z = r$. In this case, using (2.13) and (3.1), we have,

$$\begin{aligned} S_V &= \int d^6\xi \sqrt{-g} \mathcal{L}_V, \\ &= \int dx^0 dx^1 dx^2 dx^3 dw dr r^4 \left(-\frac{3}{2} Q^2 \left[\frac{1}{r^4} + f(r) \right] \right) \\ &= \int dx^0 dw dr r^4 \left(-\frac{3}{2} 2N_I \bar{q}^2 \left[\frac{1}{r^4} + f(r) \right] \right) \\ &= N_I \int dx^0 dw dr r^4 \left(-\frac{3}{2} \frac{\pi^2 \rho^4}{(r^2 + \rho^2)^{5/2}} \left[\frac{1}{r^4} + f(r) \right] \right). \end{aligned} \quad (3.4)$$

Here we find a logarithmic divergence in the integration over r . It is understood as follows:

$$\begin{aligned} S_V &\propto \int_{r_0}^{\infty} dr r^4 \left(-\frac{3}{2} \frac{\pi^2 \rho^4}{(r^2 + \rho^2)^{5/2}} \left[\frac{1}{r^4} + f(r) \right] \right) \\ &\underset{r \rightarrow \infty}{\sim} \int^{\infty} dr \left(-\frac{3}{2} \frac{\pi^2 \rho^4}{r} \right) \sim -\frac{3}{2} \pi^2 \rho^4 \log(\infty). \end{aligned} \quad (3.5)$$

This fact implies that we should reset z to other coordinate which leads to a finite energy density of the instanton.

A clue to finding such coordinate is seen in the top-down model of D4/D8 model [2, 14, 15]. In the case of the top-down model, D8 flavor brane is embedded in a set of special coordinates, which provide a flat space of r - w plane near the point $r = r_0$ by avoiding a conical singularity. This is performed in the present case by changing the coordinates from (r, w) to (z, θ) as,

$$r^5 = r_0^5 + r_0^3 z^2 \equiv k, \quad (3.6)$$

$$\theta = \frac{5}{2} w. \quad (3.7)$$

In fact, in this case, the two dimensional part of (3.1) is rewritten as

$$\begin{aligned} ds_{(2)}^2 &= r^2 f(r) dw^2 + \frac{dr^2}{r^2 f(r)} \\ &= \frac{4}{25} \left(\frac{r_0}{r} \right)^3 \left(\frac{dz^2}{r^2} + z^2 d\theta^2 \right). \end{aligned} \quad (3.8)$$

The second equation shows that the two dimensional metric is the polar coordinate of 2D flat space. Hereafter, we take $r_0 = 1$ for simplicity as in the top-down case. In this coordinate, the bulk 6D metric is written as

$$ds^2 = k^{2/5} \eta_{\mu\nu} dx^\mu dx^\nu + \frac{4}{25} k^{-3/5} (k^{-2/5} dz^2 + z^2 d\theta^2), \quad (3.9)$$

where $k = 1 + z^2$.

Here, noticing $\sqrt{-g} = (4/25)z$, the energy of the embedded instantons is given as

$$\begin{aligned} S_V &= \int dx^0 dx^1 dx^2 dx^3 dz \frac{4}{25} z \left(-\frac{3}{2} Q^2 \left[k^{-4/5} + \frac{25}{4} k^{3/5} \right] \right) \\ &= N_I \int dx^0 dz \frac{4}{25} z \left(-\frac{3}{2} \frac{\pi^2 \rho^4}{(z^2 + \rho^2)^{5/2}} \left[k^{-4/5} + \frac{25}{4} k^{3/5} \right] \right) \end{aligned} \quad (3.10)$$

where the factor $\int d\theta = 2\pi$ is absorbed to the gauge coupling constant. We can assure the finiteness of the z integration of the above action.

3.2 CS term

The baryon number is given by

$$N_B = \frac{1}{32\pi^2} \int d^3x dz \epsilon^{m_1 \dots m_4} \text{tr}(F_{m_1 m_2} F_{m_3 m_4}). \quad (3.11)$$

Then the coupling of A_0 to the baryon number is given by the following CS term,

$$\begin{aligned} S_{CS} &= \kappa_{CS} \epsilon^{m_1 \dots m_4} \int d^4x dz A_0 \text{tr}(F_{m_1 m_2} F_{m_3 m_4}) \\ &= 24\kappa_{CS} \int d^4x dz A_0 Q^2 \\ &= 48n\kappa_{CS} \int d^4x dz A_0 \bar{q}^2 \end{aligned} \quad (3.12)$$

where

$$n = \frac{N_I}{V_3}, \quad V_3 = \int d^3x = \int dx^1 dx^2 dx^3. \quad (3.13)$$

4 Effective action and the size of the instanton

The matter action with embedded instantons is obtained here as,

$$\begin{aligned} S_{\text{matter}} &= \int d^6\xi \sqrt{-g} \left(-\frac{1}{4}F^2 - \frac{1}{4}\text{tr}F_{SU(2)}^2 \right) + S_{\text{CS}} \\ &= \int d^4x dz \left(\frac{1}{2}zk^{3/5}A_0'^2 - nz\frac{12}{25}\bar{q}^2 \left[k^{-4/5} + \frac{25}{4}k^{3/5} \right] + nn_0A_0\bar{q}^2 \right), \end{aligned} \quad (4.1)$$

where $A_0' = \partial_z A_0(z)$, and $n_0 = 48\kappa_{\text{CS}}$. In order to estimate this action, we solve the equation of motion of $A_0(z)$. It is obtained as

$$-\partial_z (zk^{3/5}A_0') + nn_0\bar{q}^2 = 0. \quad (4.2)$$

Then we have

$$zk^{3/5}A_0' = \bar{d} = \frac{\pi^2}{6}nn_0 \frac{2z^3 + 3z\rho^2}{(z^2 + \rho^2)^{3/2}} + c. \quad (4.3)$$

Here, c denotes an integration constant of Eq. (4.2) over z . We take $c = 0$ to set as $\bar{d}(z=0) = 0$. Due to this condition, the matter action S_{matter} of (4.1) is written as

$$S_{\text{matter}} = \int d^4x \left\{ \mu\bar{Q} - \int dz \left(\frac{\bar{d}^2}{2zk^{3/5}} + nz\frac{12}{25}\bar{q}^2 \left[k^{-4/5} + \frac{25}{4}k^{3/5} \right] \right) \right\}, \quad (4.4)$$

where the chemical potential μ and the charge density $\bar{Q} \equiv \bar{d}(\infty)$ are given as

$$\begin{aligned} \mu &= A_0(\infty) = \int_{z_1}^{\infty} dz \frac{\bar{d}}{zk^{3/5}} + A_0(z_1) \\ &= \int_{z_1}^{\infty} dz \frac{\bar{d}}{zk^{3/5}}, \end{aligned} \quad (4.5)$$

$$\bar{Q} = \bar{d}(\infty) = \frac{\pi^2}{3}nn_0, \quad (4.6)$$

where z_1 is an arbitrary positive value and $A_0(z_1)$ is set as

$$A_0(z_1) = 0, \quad (4.7)$$

which is the boundary condition in solving the differential equation of $A_0(z)$, Eq. (4.3). Then the free energy density \mathcal{E} of the instanton system is given as

$$S_{\text{matter}} = - \int d^5\xi \mathcal{E}(\rho, \mu) \quad (4.8)$$

$$\mathcal{E}(\rho, \mu) = \int dz \left(\frac{\bar{d}^2}{2zk^{3/5}} + nz\frac{12}{25}\bar{q}^2 \left[k^{-4/5} + \frac{25}{4}k^{3/5} \right] \right) - \mu\bar{Q} \quad (4.9)$$

4.1 Size of instanton

The free energy density $\mathcal{E}(\rho, \mu)$ in (4.9) is given as a function of ρ for fixed n, n_0, z_1 . Then we find the value of $\rho = \rho_{\min}$ where $\mathcal{E}(\rho, \mu(\rho))$ takes its minimum for a set of (n, n_0, z_1) . Then for this ρ_{\min} , μ and $\mathcal{E}(\rho, \mu)$ are determined. By repeating this procedure by changing only the value n of the set (n, n_0, z_1) , we find different ρ_{\min} . As a result, we obtain the relation between μ and $\mathcal{E}(\rho, \mu)$.

We notice that the results obtained in this way depend on the other two parameters (n_0, z_1) . We give a comment related to the parameter z_1 . For $z_1 = 0$, we have a problem that the values of μ and \mathcal{E} at $\rho = 0$ are divergent:

$$\begin{aligned} \mu|_{\rho \rightarrow 0} &= \int_0^\infty dz \frac{\bar{d}(\infty)}{zk^{3/5}} \\ &\underset{z \rightarrow 0}{\sim} \bar{d}(\infty) \int_0^\infty \frac{dz}{z} \rightarrow +\infty, \end{aligned} \quad (4.10)$$

$$\mathcal{E}(\rho = 0, \mu)|_{z \rightarrow 0} \underset{z \rightarrow 0}{\sim} \int_0^\infty dz \left(-\frac{\bar{d}(\infty)^2}{2zk^{3/5}} \right) \rightarrow -\infty. \quad (4.11)$$

In the present model, these divergences are evaded by setting z_1 , the lower bound of z , at a finite value. On the other hand, in the case of the top-down model [13], there are no such divergences. In fact, we can see that μ is finite even if ρ is zero for $z_1 = 0$. Therefore, we expect the existence of some improvement of the present bottom-up model to resolve the above divergences. Here, this point is however remained as an open problem, and z_1 is introduced as a simple cutoff parameter for the above undesirable infrared divergences.

4.2 EoS for nuclear matter

By giving n, n_0, z_1 , which are the parameters of the present bottom-up model, $\mu(\rho)$ and $\mathcal{E}(\rho)$ are calculated according to the Eqs. (4.5) and (4.9) as the functions of ρ . Then a minimum point of $\mathcal{E}(\rho)$ is found at $\rho = \rho_{\min}$. Thus we can obtain $\mathcal{E}(\rho_{\min})$ and $\mu(\rho_{\min})$ for the given parameters n, n_0, z_1 .

Repeat this procedure by changing only n with (n_0, z_1) fixed, then we will get the relation of μ and \mathcal{E} . From this relation we obtain the EoS of the instanton gas as mentioned above.

In Table 1, we show a resultant example of such calculations for $n_0 = 1.5, z_1 = 0.1$. The regions of the calculations are restricted to the region for $\mu < 1.7$ [2]. On the other hand, the pressure p , which is given by $p = -\mathcal{E}$, of the instanton gas is negative for $\mu < \mu_c \sim 0.17$. So in this region, the gas is in an undesirable phase as a nuclear matter considered here. ¹

¹The negative pressure state might be constructed under a delicate balance of two kinds nuclear forces [21, 22]. Although this point is very interesting, we will discuss it in the future work.

Table 1: EoS of nuclear system at low temperature: for $n_0 = 1.5, z_1 = 0.1$ and $v_{\min} = \frac{4}{3}\pi\rho_{\min}^3 n$.

n	$\mu(\rho_{\min})$	$\mathcal{E}(\rho_{\min})$	ρ_{\min}	v_{\min}
0.005	0.0688	0.00031	0.01	2.09×10^{-8}
0.01	0.138	0.0000393	0.02	3.35×10^{-7}
0.015	0.209	-0.00022	0.03	1.70×10^{-6}
0.02	0.275	-0.00178	0.04	5.36×10^{-6}
0.03	0.411	-0.00829	0.06	2.75×10^{-5}
0.05	0.68	-0.0368	0.09	1.52×10^{-4}
0.1	1.335	-0.2075	0.13	9.2×10^{-4}

Thus we find that the stable nuclear matter exists in the region, $1.7 > \mu > \mu_c \sim 0.17$. In this region of the nuclear matter, its dilute gas picture is reasonable since $v_{\min} \sim O(10^{-4}) \ll 1$, where $v_{\min} = \frac{4}{3}\pi\rho_{\min}^3 n$ indicates the volume which is occupied by instantons in a unit 3D volume.

Here we proceed the analysis, and we can arrive at the following approximate formula

$$p = a\mu(\mu - \mu_c), \quad (4.12)$$

where $a = 0.13$ and $\mu_c = 0.17$. Then using (4.12). the energy density is given at $T = 0$ as [18]

$$\epsilon = \mu q - p = \mu \frac{\partial p}{\partial \mu} - p = a\mu^2, \quad (4.13)$$

and the speed of sound is obtained as

$$C_s^2 = \frac{\partial p}{\partial \epsilon} = \frac{\partial p / \partial \mu}{\partial \epsilon / \partial \mu} = 1 - \frac{\mu_c}{2\mu}. \quad (4.14)$$

This leads to the following bound of C_s^2 ,

$$\frac{1}{2} < C_s^2 < 1. \quad (4.15)$$

We notice that the lower bound $1/2$ is fairly large comparing to that of the ordinary nuclear matter. In this sense, the nuclear matter given here might be a special one.

Finally from (4.12) and (4.13), we arrive at the EoS of the nuclear matter given as the instanton gas. It is written as,

$$p = \epsilon - \sqrt{a\epsilon} \mu_c. \quad (4.16)$$

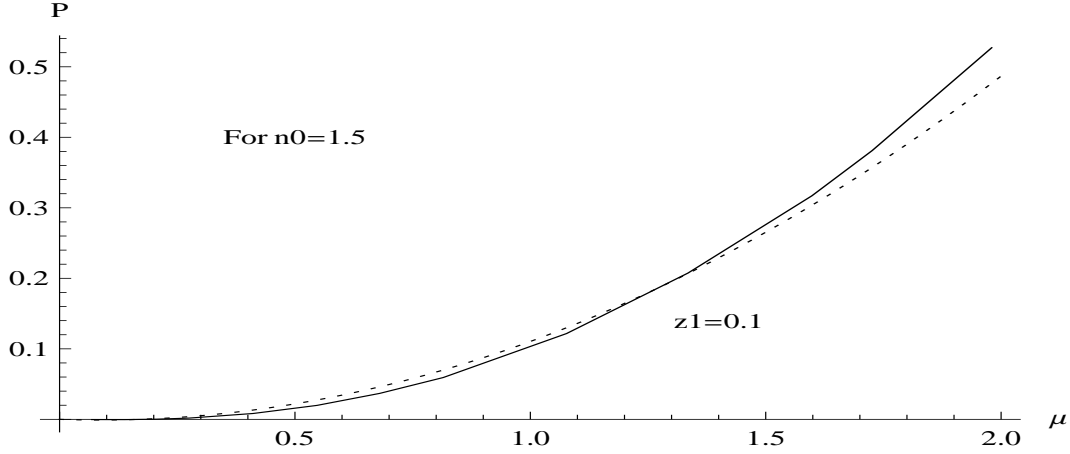


Fig. 2: $p = -\mathcal{E}(\mu)$ versus μ at stable instanton size ρ_{\min} near phase transition point $\mu_c = 0.17$. The solid curve denotes the numerical calculations, and the dotted curve represents $p = 0.13\mu(\mu - \mu_c)$.

4.3 Alternative approach to find EoS

In the present scheme, the free energy density (4.9) takes n , n_0 , ρ and z_1 as independent variables. Among them, n_0 is an intrinsic parameter of the theory and ρ is determined dynamically such that \mathcal{E} takes its minimum value, while z_1 is set to be a plausible value for the moment. The free energy density is expanded in a power series of n :

$$\mathcal{E}(n, \rho, n_0, z_1) = n c_1(\rho) - n^2 n_0^2 c_2(\rho, z_1), \quad (4.17)$$

in which

$$c_1(\rho) = \frac{12 \pi^2 \rho^4}{25 \cdot 2} \int_0^\infty dz \frac{z}{(\rho^2 + z^2)^{5/2}} \left[(1 + z^2)^{-4/5} + \frac{25}{4} (1 + z^2)^{3/5} \right], \quad (4.18)$$

$$c_2(\rho, z_1) = \left(\frac{\pi^2}{3} \right)^2 \int_0^\infty dz \frac{1}{(1 + z^2)^{3/5}} \left[\frac{1}{2} \frac{2z^2 + 3\rho^2}{(\rho^2 + z^2)^{3/2}} - \frac{1}{8} \frac{z(2z^2 + 3\rho^2)^2}{(\rho^2 + z^2)^3} \right] - \left(\frac{\pi^2}{3} \right)^2 \int_0^{z_1} dz \frac{1}{(1 + z^2)^{3/5}} \frac{1}{2} \frac{2z^2 + 3\rho^2}{(\rho^2 + z^2)^{3/2}}. \quad (4.19)$$

In order to change the independent variable from n to μ , we notice that μ can be written as

$$\mu(n, \rho, n_0, z_1) = n n_0 h(\rho, z_1) \quad (4.20)$$

with

$$h(\rho, z_1) = \frac{\pi^2}{6} \int_{z_1}^\infty dz \frac{1}{(1 + z^2)^{3/5}} \frac{2z^2 + 3\rho^2}{(\rho^2 + z^2)^{3/2}}. \quad (4.21)$$

Now, eliminating n by (4.20), the free energy density is rewritten as

$$\mathcal{E} = -\frac{c_2(\rho, z_1)}{(h(\rho, z_1))^2} \mu^2 + \frac{c_1(\rho)}{n_0 h(\rho, z_1)} \mu. \quad (4.22)$$

From the expression (4.22) one finds that the coefficients (a and b) and the critical chemical potential (μ_c) are given by

$$a = \frac{c_2(\rho, z_1)}{h(\rho, z_1)^2}, \quad b = \frac{c_1(\rho)}{n_0 h(\rho, z_1)}, \quad \mu_c = \frac{c_1(\rho) h(\rho, z_1)}{n_0 c_2(\rho, z_1)}. \quad (4.23)$$

Given μ , z_1 and n_0 , the minimum point of \mathcal{E} (i.e., the maximum point of p) in the ρ space can be sought numerically.

The minimum energy point depends on the variable which is taken fixed. Actually, two types of differential coefficients have different values as

$$\left(\frac{\partial \mathcal{E}}{\partial \rho}\right)_n - \left(\frac{\partial \mathcal{E}}{\partial \rho}\right)_\mu = \left(\frac{\partial \mathcal{E}}{\partial \mu}\right)_\rho \left(\frac{\partial \mu}{\partial \rho}\right)_n = - \left(\frac{\partial \mathcal{E}}{\partial n}\right)_\rho \left(\frac{\partial n}{\partial \rho}\right)_\mu. \quad (4.24)$$

At the point $\rho = \rho_{\min}$ such that $(\partial \mathcal{E} / \partial \rho)_n = 0$, it holds that

$$\left(\frac{\partial \mathcal{E}}{\partial \rho}\right)_\mu = - \left(\frac{\partial \mathcal{E}}{\partial \mu}\right)_\rho \left(\frac{\partial \mu}{\partial \rho}\right)_n = (-b + 2a\mu) n n_0 h_\rho(\rho, z_1). \quad (4.25)$$

In (4.25), one finds that

$$h_\rho(\rho, z_1) \equiv \frac{\partial h(\rho, z_1)}{\partial \rho} = -\frac{\pi^2}{2(2a_0)} \int_{z_1}^{\infty} dz \frac{1}{(1+z^2)^{3/5}} \frac{\rho^3}{(\rho^2+z^2)^{5/2}} < 0, \quad (4.26)$$

$$-b + 2a\mu = a(\mu - \mu_c) + a\mu > 0, \quad (4.27)$$

in the present situation, i.e., $a > 0$ and $\mu > \mu_c$. Therefore, it is concluded that

$$\left(\frac{\partial \mathcal{E}}{\partial \rho}\right)_\mu < 0 \quad (\text{at } \rho = \rho_{\min}). \quad (4.28)$$

This means that the minimum energy point along an n -fixed curve has much lower energy points towards the ρ -increasing direction with μ being kept constant. However, the problem is whether the minimum energy significantly depends on the flexed variable or not.

To estimate the difference between the two types of minimum energies, one should continue numerical calculations on \mathcal{E} from ρ_{\min} by fixing μ and by increasing ρ until one finds another minimum energy density \mathcal{E}'_{\min} . In the range of $0.015 \leq \rho \leq 0.1$ according to Table 1, the calculations make the difference of the minimum energies explicit quantitatively such as $(\mathcal{E}'_{\min} - \mathcal{E}_{\min}) / \mathcal{E}_{\min} \lesssim 0.028$.

We may consider that such differences do not affect characteristic feature of EoS, and we again employ n as the independent variable of \mathcal{E} in the succeeding sections.

5 TOV equation and M - R relation of neutron star

The TOV equations for a star with the mass m and p at the radius r in the star are given as,

$$\frac{dp}{dr} = -G(\epsilon + p) \frac{m + 4\pi r^3 p}{r(r - 2Gm)}, \quad (5.1)$$

$$\frac{dm}{dr} = 4\pi r^2 \epsilon. \quad (5.2)$$

Here, G denotes the gravitational constant. They can be solved by using the EoS given in (4.16) with the boundary condition, $p(r = 0) = p_c$ and $m(r = 0) = 0$. Solving these equations, we obtain the mass of the star, $M = m(R)$, and its radius R , where R is defined by $p(R) = 0$.

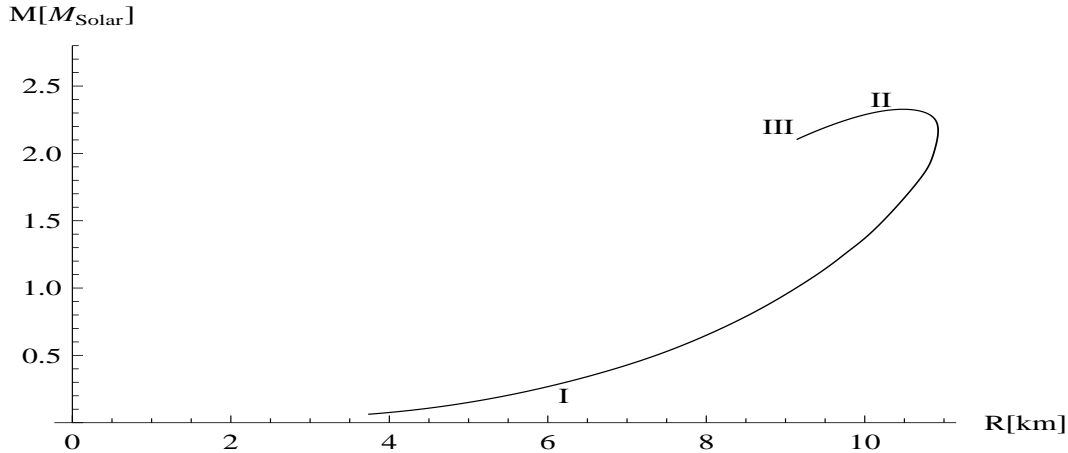


Fig. 3: Plot of the neutron mass $M(R)$ (in unit of solar mass M_\odot) versus the radius R for $p = \epsilon - \sqrt{a\epsilon}\mu_c$ (or $p = a\mu(\mu - \mu_c)$), $\mu_c = 0.17$ and $a = 0.13$.

In order to obtain the numerical results with dimensionful quantities, we must adjust the scale parameters for each dimensionful quantities (\tilde{x}). To do so, the above TOV equations are rewritten by using the dimensionless quantities as [19]

$$\frac{d\tilde{p}}{d\tilde{r}} = -B(\tilde{\epsilon} + \tilde{p}) \frac{\tilde{m} + 4\pi A\tilde{r}^3\tilde{p}}{\tilde{r}(\tilde{r} - 2B\tilde{m})}, \quad (5.3)$$

$$\frac{d\tilde{m}}{d\tilde{r}} = 4\pi A\tilde{r}^2\tilde{\epsilon}, \quad (5.4)$$

where

$$A = \frac{r_0^3 \epsilon_0}{m_0}, \quad B = \frac{Gm_0 \epsilon_0}{p_0 r_0}, \quad (5.5)$$

and the various variables (x) are replaced by the dimensionless quantities (\tilde{x}) by using its typical dimensionful value x_0 as $x = x_0 \tilde{x}$. For example, we rewrite as $p = p_0 \tilde{p}$.

Here we give a comment on the replacement, $\epsilon = \epsilon_0 \tilde{\epsilon}$ and how ϵ_0 is determined. In order to solve the TOV equation, $\epsilon(r)$ in the equation is replaced by using the Eq. (4.16) as a function of $p(r)$,

$$\epsilon = \frac{a\mu_c^2}{4} \left(1 + \sqrt{1 + \frac{4p}{a\mu_c^2}} \right)^2. \quad (5.6)$$

Similar to the above, we introduce the dimensionless quantities as $a = a_0 \tilde{a}$, $\mu_c = \mu_0 \tilde{\mu}_c$, and

$$\epsilon = \epsilon_0 \tilde{\epsilon}, \quad (5.7)$$

by imposing reasonable conditions

$$\epsilon_0 = p_0 = a_0 \mu_0^2. \quad (5.8)$$

Then in Eqs. (5.3) and (5.4), we find

$$\tilde{\epsilon} = \frac{\tilde{a}\tilde{\mu}_c^2}{4} \left(1 + \sqrt{1 + \frac{4\tilde{p}}{\tilde{a}\tilde{\mu}_c^2}} \right)^2, \quad (5.9)$$

where we put the dimensionless number as $\tilde{a}\tilde{\mu}_c^2 = 0.13 \times 0.17^2 = 3.76 \times 10^{-3}$.

Then the solutions of (5.3) and (5.4) with $A = B = 1$ are equal to the one of (5.1) and (5.2) with $G = 1$. Thus the solution of the latter equations are translated to the one of the former ones as shown in Fig. 3. It is given for $r_0 = 3.0$ km in natural unit. In this case, we find $m_0 = 2.03M_\odot$ ² and $\epsilon_0^{1/4} = 0.896$ GeV.

We can see that the radius and the mass increase with increasing p_c , the central value of the pressure. The resultant curve rotates anticlockwise toward the smaller radius in the large mass region. However from the point II to the point III in Fig. 3, the state would be unstable since $\partial M(\epsilon_c)/\partial \epsilon_c < 0$ [19]. On the other hand, in the region from I to II, we can see the behavior $\partial M(\epsilon_c)/\partial \epsilon_c > 0$. Thus, the results given here indicate the possibility of the existence of a star with $(M, R) \sim (2M_\odot, 10 \text{ km})$.

6 Comparison with the observational data

There are some important observational data which can constrain the theoretical EoS. We now have the following at least three important constraints for the M - R relation;

1. Two solar mass ($2M_\odot$) neutron star observation from the Shapiro delay measurement [23, 24].
2. Radius constraint from GW170817 via the gravitational wave observation. The actual constraint is $9.0 < R < 13.6$ km for $M = 1.4M_\odot$ [25, 26, 27].

²The symbol M_\odot denotes the solar mass.

3. Upper bound of M for cold spherical neutron stars which is estimated from no detection of relativistic optical counterpart in the analysis of GW170817. The actual limit is estimated as the range $2.15 - 2.26M_\odot$ [28].

To support $2M_\odot$ neutron stars in the theoretical calculation, we need a sufficiently stiff EoS and it is closely related to the large value of the speed of sound. Then, the pressure of matter in the inner neutron star core should be large. From the second constraint that the radius is relatively small in the moderate M region, it requires that the pressure of matter in the outer neutron core should be relatively small. It is interesting that our bottom-up model is quite simple, but our EoS can manifest the $2M_\odot$ constraint and the restriction that the M - R curve must go through $9.0 < R < 13.6$ around $M \sim 1.4M_\odot$. However, too stiff EoS is not preferable because of the third constraint. Unfortunately, the maximum mass M_{\max} overshoots the $2.15 - 2.26M_\odot$ constraint, but we can expect that there are some phase transitions at high density such as the chiral, deconfined, and color superconducting phase transitions which we do not consider in this study. Then, EoS can be softer than the present one at high density and thus M_{\max} should be smaller than the present value. Particularly, EoS becomes soft if there is a first-order phase transition; for example, see Ref. [29].

It should be noted that the above constrains can restrict the large and moderate M regions, but the lower M region is not restricted so much. Of course, there are several nuclear theoretical EoS and thus we can qualitatively discuss the lower M region where the low density part of EoS dominates the M - R curve. With our EoS, the M - R curve flows down to the left bottom, but several M - R curves with different EoS flow down to the right bottom. This result may be induced from the fact that our C_s^2 cannot be less than $1/2$ even in the sufficiently low density region. Such behavior is similar to the M - R curves obtained with EoS proposed in Ref. [30]; the actual behavior of the curves can be seen in Refs. [31, 32] denoted as ‘‘SQM1-3’’; these EoS which contain the quark matter make self-bounded neutron stars which do not have minimum masses. The tendency of the M - R curves in the small M region in our model may be modified when we suitably introduce ‘‘interactions’’ to the present model because we employ the dilute instanton gas approximation; the baryonic contribution can be expected to have relatively strong effects on EoS at low density. In addition, we here use the dilute gas of the instanton of the $SU(2)$ gauge field and thus the number of the flavor is considered as two; the system contains the up and down quarks and thus there is no strange quark. This may introduce the unclearness to the present M - R curves because the EoS will be softer than the present one if hyperons appear in the system; since the core of the neutron star is very dense, the hyperon degree of freedom can join the game as the baryonic mode in addition to nucleons. This softening problem induced by the hyperons is the so-called hyperon puzzle which is a long standing problem in the study of the neutron stars with EoS; see Ref. [33] as an example. To discuss this problem in the present bottom-up holographic model, we must consider differences between the light quarks and the strange quark, interactions and bound states more deeply. Improvements for above problems are our future work.

7 Summary and discussions

In this paper, we have studied cold nuclear matter and its equation of state (EoS) based on the six dimensional holographic model, which was investigated to realize the color superconducting phase of QCD previously. The nuclear matter was introduced as a dilute gas of deformed instantons in the AdS soliton background. The instantons are made of the $SU(2)$ gauge fields and the action includes the Chern-Simons term as well as the kinetic term. Owing to the energy balance between these two terms in the action, the size of the instanton can be determined for fixed parameters of the model. As the result, EoS for nuclear matter, *i.e.*, pressure as a function of energy density, is obtained. Through the evaluation of the instanton size, it turns out that number of instantons in a unit volume is very small so that our dilute gas picture is consistent. Furthermore, there exists a critical value for the chemical potential below which the pressure gets negative. The EoS obtained here is very stiff because the speed of sound $C_s^2 > \frac{1}{2}$. This is very specific to our model.

Then, we applied the EoS to solve the Tolman-Oppenheimer-Volkov equations for a compact star numerically and found the mass-radius (M - R) relationship. The curve is somewhat similar to the one for strange quark matter in Refs. [30, 32] and we provided a certain interpretation for that. Our result is compared with the observational data and it is seen that the maximum mass overshoots the current constraint since our EoS for the nuclear matter is very stiff. This might suggest that we have more phases such as quark matter, which softens the current EoS, than that of the nuclear matter.

In order to improve our current study, several ingredients are taken into account. One is to go beyond the dilute gas approximation of instantons. By doing this, our EoS is modified and eventually the M - R curve might be changed so as to be more consistent with the observational data. The other is to study whether the system enjoys the phase transition from nuclear matter to (perhaps color superconducting) quark matter at higher baryon density. If such a phase transition is present, the EoS gets soften and the resultant M - R curve could be modified. Furthermore it will be interesting to extend our current study into the case with hyperon degrees of freedom. To this end, the holographic treatment of heavy-light meson system (for instance, see [34]) must be instructive. These will be the future issues.

Acknowledgments

We are grateful to Masayuki Matsuzaki for useful discussions on the neutron stars and TOV equations.

References

- [1] Pallab Basu, Fernando Nogueira, Moshe Rozali, Jared B. Stang, Mark Van Raamsdonk, “Towards A Holographic Model of Color Superconductivity”, New J.Phys.13:055001,2011, [arXiv:1101.4042 [hep-th]].
- [2] Kazuo Ghoroku, Kouji Kashiwa, Yoshimasa Nakano, Motoi Tachibana, Fumihiko Toyoda “Color Superconductivity in Holographic SYM Theory”, Phys. Rev. D 99, 106011 (2019), arXiv:1902.01093[hep-th]:
- [3] Steven S. Gubser, “Breaking an Abelian gauge symmetry near a black hole horizon”, Phys.Rev.D78:065034,2008, arXiv:0801.2977 [hep-th].
- [4] Sean A. Hartnoll, Christopher P. Herzog, Gary T. Horowitz, “Building an AdS/CFT superconductor”, Phys. Rev. Lett. 101.031601, [Xiv:0803.3295 [hep-th]];
- [5] S. A. Hartnoll, C. P. Herzog and G. T. Horowitz, “Holographic Superconductors,” JHEP **0812**, 015 (2008) [arXiv:0810.1563 [hep-th]].
- [6] Tatsuma Nishioka, Shinsei Ryu, Tadashi Takayanagi, “Holographic Superconductor/Insulator Transition at Zero Temperature”, JHEP 1003:131,2010, JHEP03(2010)131, [arXiv:0911.0962 [hep-th]].
- [7] N. Iqbal, H. Liu, M. Mezei *et al.*, “Quantum phase transitions in holographic models of magnetism and superconductors,” Phys. Rev. **D82**, 045002 (2010). [arXiv:1003.0010 [hep-th]].
- [8] Andrew Chamblin, Roberto Emparan, Clifford V. Johnson, Robert C. Myers, “Charged AdS Black Holes and Catastrophic Holography”, 10.1103/PhysRevD.60.064018, hep-th/9902170:
- [9] Kazem Bitaghsir Fadafan, Jesus Cruz Rojas, Nick Evans, “A Holographic Description of Colour Superconductivity”, Phys. Rev. D 98, 066010 (2018), [arXiv:1803.03107 [hep-ph]].
- [10] Cao H. Nam, “A more realistic holographic model of color superconductivity in Einstein-Gauss-Bonnet gravity”, arXiv:2101.00882[hep-th]
- [11] Oren Bergman, Gilad Lifschytz, Matthew Lippert, “Holographic Nuclear Physics”, JHEP0711:056,2007, arrXiv:0708.0326 [hep-th] :
- [12] M. Rozali, H. -H. Shieh, M. Van Raamsdonk and J. Wu, “Cold Nuclear Matter In Holographic QCD,” JHEP **0801**, 053 (2008) [arXiv:0708.1322 [hep-th]].
- [13] Kazuo Ghoroku, Kouki Kubo, Motoi Tachibana, Tomoki Taminato, Fumihiko Toyoda, “Holographic cold nuclear matter as dilute instanton gas”, Phys-RevD.87.066006, arXiv:1211.2499 [hep-th].

- [14] T. Sakai and S. Sugimoto, “Low energy hadron physics in holographic QCD,” *Prog. Theor. Phys.* **113**, 843 (2005) [hep-th/0412141].
- [15] H. Hata, T. Sakai, S. Sugimoto and S. Yamato, “Baryons from instantons in holographic QCD,” *Prog. Theor. Phys.* **117**, 1157 (2007) [hep-th/0701280 [HEP-TH]].
- [16] Florian Preis and Andreas Schmitt, “Layers of deformed instantons in holographic baryon matter”, *J. High Energ. Phys.* (2016) 2016, arXiv:1606.00675 [hep-ph].
- [17] Carlos Hoyos, David Rodriguez Fernandez, Niko Jokela, Aleksi Vuorinen “Holographic quark matter and neutron stars”, *Phys. Rev. Lett.* **117**, 032501 (2016), arXiv:1603.02943 [hep-ph].
- [18] Kazem Bitaghsir Fadafan, Jesus Cruz Rojas, Nick Evans “Deconfined, Massive Quark Phase at High Density and Compact Stars: A Holographic Study”, *Phys. Rev. D* **101**, 126005 (2020), arXiv:1911.12705 [hep-ph]
- [19] Kazem Bitaghsir Fadafan, Jesus Cruz Rojas, Nick Evans, “Holographic quark matter with colour superconductivity and a stiff equation of state for compact stars”, *Phys. Rev. D* **103**, 026012 (2021) [arXiv:2009.14079 [hep-ph]].
- [20] E. Witten, “Anti-de Sitter space, thermal phase transition, and confinement in gauge theories,” *Adv. Theor. Math. Phys.* **2** (1998) 505 [arXiv:hep-th/9803131].
- [21] M. Berthelot, *Ann. Chim. Phys.* **30** (1850) 332.
- [22] Thomas D. Cohen, Scott Lawrence, Yukari Yamauchi, “The thermodynamics of large-N QCD and the nature of metastable phases”, *Phys. Rev. C* **102**, 065206 (2020), arXiv:2006.14545 [hep-ph].
- [23] P. Demorest, T. Pennucci, S. Ransom, M. Roberts and J. Hessels, *Nature* **467**, 1081-1083 (2010) doi:10.1038/nature09466 [arXiv:1010.5788 [astro-ph.HE]].
- [24] J. Antoniadis, P. C. C. Freire, N. Wex, T. M. Tauris, R. S. Lynch, M. H. van Kerkwijk, M. Kramer, C. Bassa, V. S. Dhillon and T. Driebe, *et al.* *Science* **340**, 6131 (2013) doi:10.1126/science.1233232 [arXiv:1304.6875 [astro-ph.HE]].
- [25] E. Annala, T. Gorda, A. Kurkela and A. Vuorinen, *Phys. Rev. Lett.* **120**, no.17, 172703 (2018) doi:10.1103/PhysRevLett.120.172703 [arXiv:1711.02644 [astro-ph.HE]].
- [26] S. De, D. Finstad, J. M. Lattimer, D. A. Brown, E. Berger and C. M. Biwer, *Phys. Rev. Lett.* **121**, no.9, 091102 (2018) [erratum: *Phys. Rev. Lett.* **121**, no.25, 259902 (2018)] doi:10.1103/PhysRevLett.121.091102 [arXiv:1804.08583 [astro-ph.HE]].
- [27] I. Tews, J. Margueron and S. Reddy, *Phys. Rev. C* **98**, no.4, 045804 (2018) doi:10.1103/PhysRevC.98.045804 [arXiv:1804.02783 [nucl-th]].

- [28] M. Shibata, S. Fujibayashi, K. Hotokezaka, K. Kiuchi, K. Kyutoku, Y. Sekiguchi and M. Tanaka, *Phys. Rev. D* **96**, no.12, 123012 (2017) doi:10.1103/PhysRevD.96.123012 [arXiv:1710.07579 [astro-ph.HE]].
- [29] T. Kojo, *AAPPS Bull.* **31**, no.1, 11 (2021) doi:10.1007/s43673-021-00011-6 [arXiv:2011.10940 [nucl-th]].
- [30] M. Prakash, J. R. Cooke and J. M. Lattimer, *Phys. Rev. D* **52**, 661-665 (1995) doi:10.1103/PhysRevD.52.661
- [31] J. M. Lattimer and M. Prakash, *Astrophys. J.* **550**, 426 (2001) doi:10.1086/319702 [arXiv:astro-ph/0002232 [astro-ph]].
- [32] F. Ozel, D. Psaltis, T. Guver, G. Baym, C. Heinke and S. Guillot, *Astrophys. J.* **820**, no.1, 28 (2016) doi:10.3847/0004-637X/820/1/28 [arXiv:1505.05155 [astro-ph.HE]].
- [33] W. Weise, *JPS Conf. Proc.* **26**, 011002 (2019) doi:10.7566/JPSCP.26.011002 [arXiv:1905.03955 [nucl-th]].
- [34] J. Erdmenger, K. Ghoroku and I. Kirsch, “Holographic heavy-light mesons from non-Abelian DBI,” *J. High Energ. Phys.* 09 (2007) 111, doi:10.1088/1126-6708/2007/09/111 [arXiv:0706.3978 [hep-th]].